Inorganic Chemistry

ARTICLE

pubs.acs.org/IC

Comparison of the Spectroscopic Properties of π-Conjugated, Fused Salphen Triads Embedded with Zn-Homo-, Ni-Homo-, and Ni/Zn-Heteronuclei

Hirohiko Houjou,* Muneyuki Ito, and Koji Araki

Institute of Industrial Science, The University of Tokyo, 4-6-1 Komaba, Meguro-ku, Tokyo 153-8505, Japan

Supporting Information

ABSTRACT: Stepwise condensation reactions of 2,6-dihydroxynaphthalene-1,5-dicarbaldehyde and a phenylenediamine with concomitant binding of metal ions afforded a trinuclear complex of a fully π-conjugated, fused salphen ligand. By changing the synthetic pathway, we obtained a series of homo- and heteronuclear complexes containing selected combinations of nickel(II) and zinc(II) ions. Comparison of the trinuclear complexes' spectroscopic features with those of analogous dinuclear complexes revealed that the absorption spectrum of each trinuclear complex is composed of a salphen-centered absorption at 400 nm and a naphthalene-centered absorption around 500−600 nm, suggesting that the π-conjugated system is divided into several compartments, each of which independently undergoes electronic excitation. Molecular orbital calculations revealed that the formal fusion of the salphen moieties increases the highest occupied molecular orbital (HOMO) level by ∼0.4 eV, which in turn causes the low-energy absorption observed in the spectra. In contrast, interorbital interactions mediated by the N_2O_2 metal coordination site are small, even though this site is bridged by an *o*-phenylene linkage. These results suggest that the coordination site effectively breaks electronic communication between the compartments, which in turn affect various spectroscopic properties of the π-conjugated metallo-polysalphens.

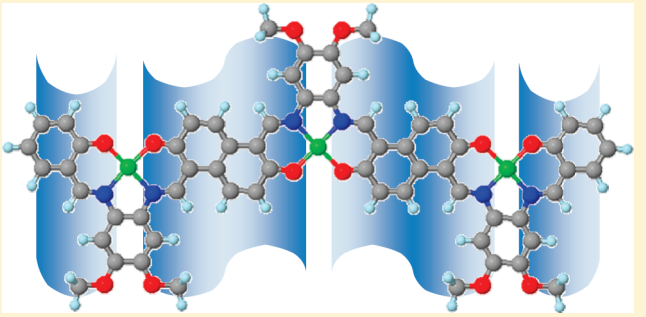

INTRODUCTION

Interest in arranging metal atoms with various electronic and magnetic properties has been growing in connection with the recent development of metal clusters, metal−organic frameworks, metallo-supramolecular polymers, and other metal-containing materials.[1−4] Conjugated metallopolymers, in which metal atoms are directly bound to an organic polymer chain with extended π-conjugation, are of special interest[5−8] because these systems are expected to exhibit various properties innate to π-conjugated systems such as conductivity, redox activity, photoluminescence, and magnetism. As a result of metal binding to a conjugated polymer ligand, the electronic state of the metal couples with that of the ligand's π-system, affording such interesting phenomena as metallo-aromaticity and valence tautomerism.[9−12] The formation of Schiff-base linkages has been utilized as a promising means to synthesize π-conjugated frameworks.[13−16] The imine nitrogen atom serves as a good donor for metal ions, giving rise to additional effects like shape-persistence that originate from the structural rigidity induced by coordination bonding between the metal ion and imine nitrogen. Several recent publications have reported the observation of these effects in fully π-conjugated oligo-nuclear salens (salen = *N*,*N*-disalicylidene ethylenediamine) and salphens (salphen = *N*,*N*-disalicylidene phenylenediamine).[17−19] In addition, several reports have described the synthesis of metallo-polysalens and -salphens with π-conjugated linkers between the coordination sites by means of polycondensation,[20,21] cross-coupling,[22] and electrolytic polymerization.[23,24] Among these synthetic routes, the condensation of an aldehyde and amine is of particular interest, since this reaction may afford polymers via reversible formation of a Schiff-base linkage with concomitant binding of a metal ion to the resultant coordination site.[25]

Despite the synthetic efforts mentioned above, a standard protocol for the design of poly salens/-salphens exhibiting electronic functions that arise from electronic interactions between metal-atom coordination sites and π-conjugated systems has not yet been achieved. Further studies of the electronic interaction mechanisms and their contributions to the improvement of electronic functions are needed. We anticipated that the fusion of the aromatic rings of a salen or salphen will bring about a strong interaction between coordination sites by minimizing complicated effects arising from torsion of single bonds in the linker unit. To construct fused salphens, we chose 2,6-dihydroxynaphthalene-1,5-dicarbaldehyde (**1**) as a constitutional isomer.[26] This compound was first introduced by Dewar, who reported that some coordination

Received: April 19, 2011
Published: May 10, 2011

polymers of the dioxime of **1** exhibit semiconductor performance.[27] Despite this promising observation, the Schiff-base chemistry of this aldehyde has not been explored extensively. Recently, we have synthesized various homo- and heterodinuclear salphen complexes with **1**.[28] We observed some substantial changes in the dinuclear complexes' spectral profiles as compared to those of the corresponding mononuclear complexes. Spectroscopic analysis of a series of heterodinuclear salphens has revealed absorption bands originating from the intrinsic salphen complex unit and from a new π-conjugated system generated by an ideal cata-condensation of salphen units.[28b] We expect that increasing the number of salphen units in the complexes from two to three would enable us to evaluate the effect of extensive π-conjugation on the electronic state of the whole metal−organic system. In this paper, we report the preparation of homo- and heterotrinuclear complexes of a fully conjugated, fused salphen ligand with selected combinations of nickel(II) and zinc(II) ions, and we describe the spectroscopic properties of the complexes from both experimental and theoretical viewpoints. These results provide key molecular design information to enable the realization of π-conjugated metallo-polysalphens.

EXPERIMENTAL SECTION

General Procedures. All chemicals and solvents were purchased from Tokyo Kasei Kogyo (TCI) and were used without further purification. Dialdehyde **1** and 4,5-didodecyloxyphenylene-1,2-diamine (**2**) were prepared according to the procedures reported previously.[26,29] UV−vis absorption spectra of a pyridine (spectroscopic grade, 2×10^{-6} M) solution of each solute were acquired with a JASCO V-630 spectrophotometer. NMR spectra were recorded on a JEOL JNM-ECS400 instrument (400 MHz for ^{1}H). FT-IR spectra were recorded with a Shimadzu FTIR-8700 instrument.

Synthesis. *Zn_3L3.* The mononuclear complex ligand ZnL1 was prepared as reported previously.[28b] ZnL1 (39.0 mg, 46 μmol) and **2** (10.9 mg, 23 μmol) were dissolved in dimethylformamide (DMF, 15 mL), to which a methanolic solution of zinc(II) acetate dihydrate (5.2 mg, 23 μmol in 4 mL) was added. The mixture was left without stirring for 24 h at 25 °C, and then the precipitate was collected by filtration. Methanol (15 mL) was added to the filtrate to afford a second precipitate, which was collected by filtration. The product Zn_3L3, a reddish brown solid, was obtained at a yield of 41.0 mg (82%). IR (KBr): ν = 1609 ($\nu_{C=N}$), 1268 (ν_{C-O}), 548 (ν_{O-Zn}), 496 (ν_{N-Zn}) cm^{-1}. MS (FAB+): *m/z* 2185.6 (calcd. for M$^+$ 2183.1 (exact), 2186.1 (100%)). $C_{128}H_{178}N_6O_{12}Zn_3 \cdot 3H_2O$ (2243.03): calcd. C 68.54, H 8.27, N3.75; found C 68.26, H 8.42, N 3.68. ^{1}H NMR ([D_5] pyridine): δ = 0.89 (t, ^3J = 6.8 Hz, 18H, CH_3), 1.20−1.39 (m, 96H, $-CH_2-$), 1.48−1.56 (m, 12H, $-CH_2-$), 1.77−1.89 (m, 12H, $-CH_2-$), 4.09 (t, ^3J = 6.0 Hz, 4H, $-CH_2O-$), 4.14−4.18 (m, 8H, $-CH_2O-$), 6.70 (t, ^3J = 7.5 Hz, 2H, Ar*H*), 7.41 (d, ^3J = 7.5 Hz, 2H, Ar*H*), 7.44 (t, ^3J = 7.5 Hz, 2H, Ar*H*), 7.55 (d, ^3J = 10.0 Hz, 4H, Ar*H*), 7.57 (d, ^3J = 7.5 Hz, 2H, ArH), 7.69 (s, 2H, Ar*H*), 7.90 (s, 2H, ArH), 7.91 (s, 2H, Ar*H*), 8.83 (d, ^3J = 10.0 Hz, 4H, Ar*H*), 9.30 (s, 2H, ArH), 10.18 (s, 2H, $-CH$=N-), 10.20 (s, 2H, $-CH$=N-).

NiZnNiL3. Mononuclear complex ligand NiL1 was prepared as reported previously.[28b] NiL1 (38.4 mg, 46 μmol) and **2** (10.9 mg, 23 μmol) were dissolved in chloroform (10 mL), to which a methanolic solution of zinc(II) acetate dihydrate (5.2 mg, 23 μmol in 2 mL) was added. The mixture was stirred at 60 °C for 24 h, and then the precipitate, a reddish brown solid, was collected by filtration. The product was obtained at a yield of 50 mg (99%). IR (KBr): ν = 1607 ($\nu_{C=N}$), 1281 (ν_{C-O}), 516 (ν_{O-M}), 457 (ν_{N-M}) cm^{-1}. MS (FAB$^+$): *m/z* 2172.3 (calcd. for M+ 2171.1 (exact), 2172.2 (100%)). $C_{128}H_{178}N_6O_{12}Ni_2Zn \cdot 2H_2O$ (2229.64): calcd. C 69.51, H 8.29, N3.80; found C 69.36, H 8.34, N 4.03.

Scheme 1. Synthesis of the Trinuclear Complex $M_aM_bM_aL3$

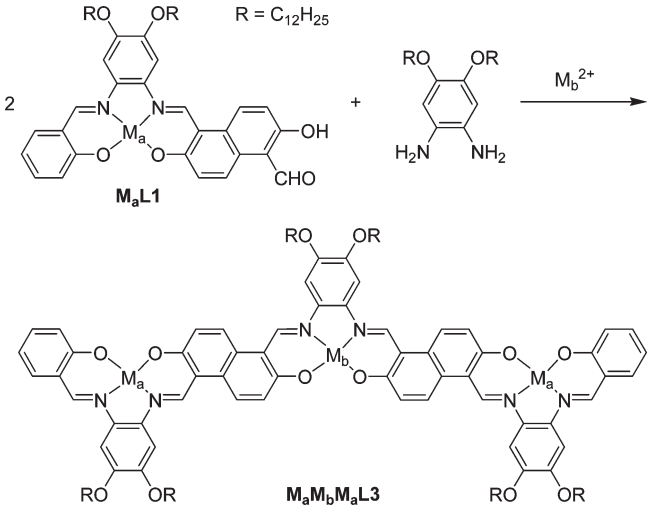

Ni_3L3. The trinuclear zinc complex Zn_3L3 (30.7 mg, 14 μmol) was dissolved in a mixture of DMF and pyridine (v/v = 25 mL/3 mL), to which a DMF solution of nickel(II) acetate tetrahydrate (10.6 mg, 43 mmol in 2 mL) was added. The mixture was stirred for 12 h at 60 °C, and then the precipitate, a dark brown solid, was collected by filtration. The product was obtained at a yield of 24.0 mg (80%). IR (KBr): ν = 1603 ($\nu_{C=N}$), 1286 (ν_{C-O}), 542 (ν_{O-Ni}), 457 (ν_{N-Ni}) cm^{-1}. MS (FAB+): *m/z* 2168.3 (calcd. for M$^+$ 2165.2 (exact), 2168.2 (100%)). $C_{128}H_{178}N_6O_{12}Ni_3 \cdot 3H_2O$ (2219.19): calcd. C 69.16, H 8.34, N3.78; found C 69.62, H 8.26, N 3.98.

Calculations. Ab initio calculations were performed using Gaussian03w software.[30] The geometry of each compound was optimized by means of the Hartree−Fock method using the 6-31G(d) basis set. For thus-obtained structures, semiempirical singly excited configuration interaction (SCI) calculations were performed using the ZINDO/1[31] subroutine incorporated in Gaussian03w. The lowest 15 and 20 singlet excited states were calculated by direct-CI algorithm[32] for dinuclear and trinuclear complexes, respectively. The molecular orbital coefficients were visualized with the Jmol 12.0.15 software.[33]

RESULTS AND DISCUSSION

Synthesis of the Complexes. Scheme 1 shows the preparation of a trinuclear complex represented as $M_aM_bM_aL3$. When zinc(II) was used as both M_a and M_b, the reaction proceeded under relatively mild conditions and afforded a good yield of homotrinuclear zinc complex Zn_3L3. In a similar reaction for the preparation of homotrinuclear nickel complex Ni_3L3, however, the reaction was inefficient; the yield was at most 11%, even after prolonged heating. We then prepared Ni_3L3 from Zn_3L3 via trans-metalation reactions (Scheme 2), and the product was obtained at a yield of 80%, which reflected the reactions' efficiency as reported by Kleij et al.[19] As anticipated, the UV−vis spectra of Ni_3L_3 obtained by two different reaction pathways were substantially identical (Supporting Information, Figure S1). We have already confirmed the efficiency of analogous reactions for a dinuclear zinc complex, which converts to the corresponding nickel or copper complexes.[28] These results also suggest that this synthetic protocol restricts M_a and M_b to Ni and Zn, respectively, to avoid unfavorable trans-metalation. Starting from NiL1, phenylenediamine, and zinc(II) acetate, we obtained the heterotrinuclear complex NiZnNiL3 at a high yield (99%). It was

dx.doi.org/10.1021/ic200798d |*Inorg. Chem.* 2011, 50, 5298–5306

Scheme 2. Nonreversible Trans-Metallation Reactions for an L3 Ligand Complex

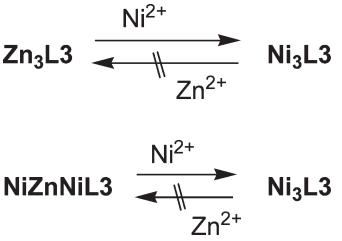

Table 1. Comparison of ^{1}H NMR Chemical Shifts of Selected Protons in the Labeled Regions Shown in Figure *1*

		chemical shift (ppm)			
		H_a	H_b	H_e	H_f
Zn_3L3	A	7.57	7.44	9.30	7.69
	B, C	7.55	8.83	10.18	7.90
		7.55	8.83	10.20	7.91
Zn_2L2	A	7.55	7.44	9.29	7.68
	B	7.53	8.80	10.16	7.89

also confirmed that NiZnNiL3 was converted to Ni_3L3 by refluxing in the presence of nickel(II) acetate, which induced trans-metalation (Scheme 2).

Table 1 lists the ^{1}H NMR chemical shifts of selected signals for Zn_3L3 and Zn_2L2 (spectra were shown in Supporting Information, Figure S2). For convenience of comparing the signals, we divided the complex into three compartments: A, B, and C, which correspond to the respective labeled sections of the molecules shown in Figure 1. The azomethine protons (H_e) in compartments A, B, and C are all nonequivalent. The two signals in the low-field region (10.18 and 10.20 ppm) were attributed to the azomethine protons in parts B and C, where atoms at the periposition of the naphthalene ring may exert some steric effects. As for the aromatic ring in compartment B of Zn_3L3, protons H_a and H_b were hardly distinguishable from the H_a and H_b protons in compartment C of Zn_3L3. In addition, the chemical shifts of these aromatic protons were quite similar to those of the corresponding protons in compartment B of Zn_2L2 (Table 1). These observations suggest that the electronic state of the naphthalene ring is governed by local C_{2h} symmetry. In other words, the local electronic state around the naphthalene ring in Zn_3L3 is approximately the same as that in dinuclear complex Zn_2L2.

The ^{1}H NMR spectra of trinuclear complex NiZnNiL3 gave only a series of broadened peaks in the region for alkyl protons. This observation is consistent with the results obtained for the dinuclear complexes Ni_2L2 and NiZnL2, which gave similar broadened spectra due partly to their potential magnetism. Unfortunately, the trinuclear complexes Ni_3L3 did not produce any recognizable spectra, because of its poor solubility. The FAB (positive mode) mass spectra showed only small peaks corresponding to the trinuclear complex, while there were some extra peaks that imply demetalation, and so on (Supporting Information, Figure S3). To characterize Ni_3L3 and NiZnNiL3, as well as Zn_3L3, we compared their FT-IR spectra (Figure 2). The overall similarity of the peaks in the stretching and bending vibration

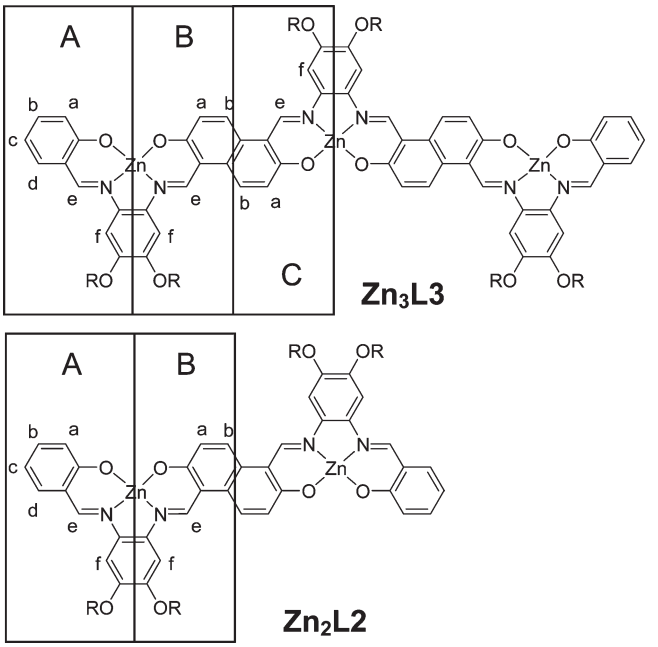

Figure 1. Compartment of di- and trinuclear complexes for ^{1}H NMR analysis.

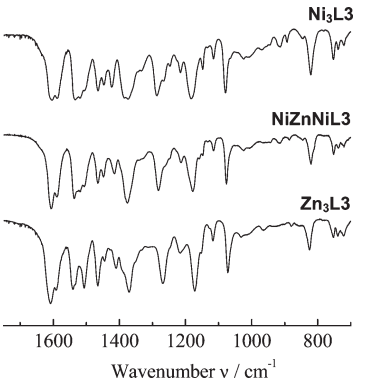

Figure 2. FT-IR spectra of the homo- and heterotrinuclear complexes.

bands suggests that Ni_3L3 and NiZnNiL3 have essentially the same framework as that confirmed for Zn_3L3. The slight differences observed for several bands around 1500 cm^{-1} seem to reflect a difference in the arrangement of metals. Interestingly, the IR spectrum of the heterotrinuclear complex shows a profile intermediate between the profiles of the homo nickel and homo zinc triads, but not a simple superposition of them.

UV−vis Spectra. Figure 3a shows the UV−vis spectrum of trinuclear complex Ni_3L3 together with that of the corresponding dinuclear complex Ni_2L2. For each spectrum, the absorption coefficients were normalized by the number of metal ions per molecule. Both spectra show intense bands around 400 nm and moderate bands around 500−600 nm. As discussed later in this report, these spectral features are common for all the complexes prepared herein, suggesting that these absorption bands arise mainly from the $\pi-\pi^*$ transition in the ligand, although there may be a small contribution from charge transfer between the metal and the ligand. The normalized absorbances of the two spectra are quite similar to each other, suggesting that the overall intensity of each spectrum is roughly proportional to the number

dx.doi.org/10.1021/ic200798d |*Inorg. Chem.* 2011, 50, 5298–5306

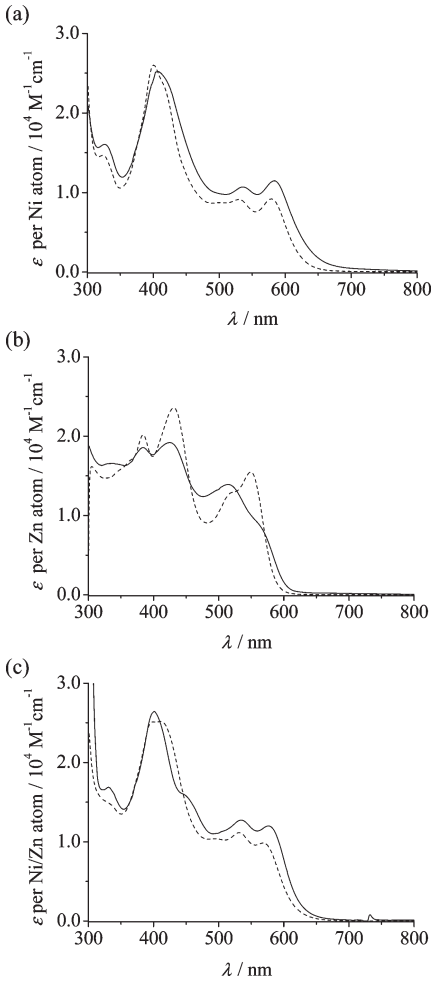

Figure 3. UV−vis absorption spectra of trinuclear (solid line) and dinuclear (dashed line) complexes: (a) Ni_3L3 and Ni_2L2, (b) Zn_3L3 and Zn_2L2, and (c) NiZnNiL3 and NiZnL2. Absorption coefficients are normalized by the number of metal atoms per molecule.

of salphen units within the complex. However, the normalized absorbance of the trinuclear complex at 500−600 nm is about 1.25 times as large as that of the dinuclear complex. The origins of the two bands in this region were assigned based on observations for a series of dinuclear salphen complexes that have the same naphthalene moiety:[28] the shorter-wavelength band was concluded to have originated from the absorption innate to the salphen moiety, whereas the longer-wavelength band was attributed to the absorption innate to an additional π-electronic system generated by the formal fusion of the aromatic rings. This assignment was verified in terms of quantum chemistry (vide infra).

The apparent coincidence of the spectra around 400 nm suggests that there are no significant interactions among the salphen units through the π-conjugated system of naphthalene. However, this result does not necessarily mean that the whole spectrum is composed of contributions from the individual salphen units, as evidenced by the absorption at 500−600 nm. The intensity ratio of trinuclear complex to dinuclear complex in this region is 1.25, which is close to 1.33 (= 0.667/0.500), the number ratio of naphthalene moieties per nickel atom between the two complexes. Consequently, the spectrum of Ni_3L3 can be interpreted as a superposition of the contribution from three salphen units and two naphthalene moieties. While the observed intensity is rather smaller than the predicted one, the band of Ni_3L3 at 500−600 nm is slightly red-shifted and significantly broadened compared to that of Ni_2L2, implying the substantial effect of the elongation of the π-conjugated system. These results indicate that the origin of the band around 500−600 nm can be identified as a local excitation at the bis-metalated Schiff base of 2,6-dihydroxynaphthalene-1,5-dicarbaldehyde.

Similarly, the spectra of Zn_3L3 and Zn_2L2 exhibit an intense band around 400 nm and a moderate band around 500−600 nm (Figure 3b). The two broad absorption bands are again attributable to the absorption innate to a salphen unit and to a naphthalene moiety, respectively. Although the normalized absorption of Zn_3L3 is slightly reduced compared to that of Zn_2L2, the overall similarity between the two profiles indicates that the interpretation applied to nickel complexes also applies here; that is, that the change in absorption observed for Zn_3L3 is caused by the extension of π-conjugation relative to that observed for the dinuclear complex. In addition, a significant broadening of the absorption band around 500−600 nm suggests that the delocalization of π-electrons along the elongated conjugated system was more pronounced in the zinc complex than it was in the trinuclear nickel complex.

Figure 3c shows the absorption spectrum of the heterotrinuclear complex NiZnNiL3 (solid line). The spectrum has an intense band at 400 nm and a moderate band around 500−600 nm. On the basis of the above discussion, we can assume that the former band is composed of the contribution from the two nickel complexes and one zinc complex with the salphen ligands. The latter band shows a line shape intermediate between the shapes of the trinickel and trizinc complexes, implying that the band is attributable to the absorption innate to a nickel−zinc heteronuclear complex of 2,6-dihydroxynaphthalene-1,5-diimine. Thus, comparing this spectrum with that of a nickel−zinc heterodinuclear complex is meaningful. Figure 3c superimposes the spectrum of NiZnL2 (dotted line) on that of the trinuclear complex. In the region of 500−600 nm, the profiles of NiZnL2 and NiZnNiL3 are quite similar to each other, with the latter being about 1.22 times as intense as the former. This result is consistent with that observed for the nickel homotrinuclear complex.

Previously, we reported a detailed study on the electronic state of 2,6-dihydroxynaphthalene carbaldehydes, revealing that their lowest-energy electronic transition can be simply described as an electronic reorganization between covalent and ionic structures of the resonance hybrid (Scheme 3a).[26] The energy difference between the ground and excited states is considerably influenced by the position of the formyl group, which increases the contribution of the ionic structure to the ground state through resonance-assisted hydrogen bonding (RAHB).[34−36] According to recent theoretical analyses, RAHB is interpreted as the modification of π-orbitals' energy by a proton-bridged, quasi six-membered ring, rather than the modification of the strength of hydrogen bonding by the adjacent π-electronic system.[26,37,38] This interpretation is seemingly applicable to a metal-bridged six-membered ring.[39,40] Accordingly, we can interpret the absorption of the fused salphen complexes based on a resonance hybrid shown in Scheme 3b. Notably, different Kekulé structures can be drawn for each compartment (A, B, and C) shown in Figure 1. In other words, this resonance hybrid scheme implies that each compartment can independently undergo excitation. This classical interpretation reasonably accounts for the spectroscopic features

dx.doi.org/10.1021/ic200798d |*Inorg. Chem.* 2011, 50, 5298–5306

Scheme 3. Resonance Structures of (a) 2,6-Dihydroxynaphthalene-1,5-dialdehyde and (b) Its Schiff-Base Complex

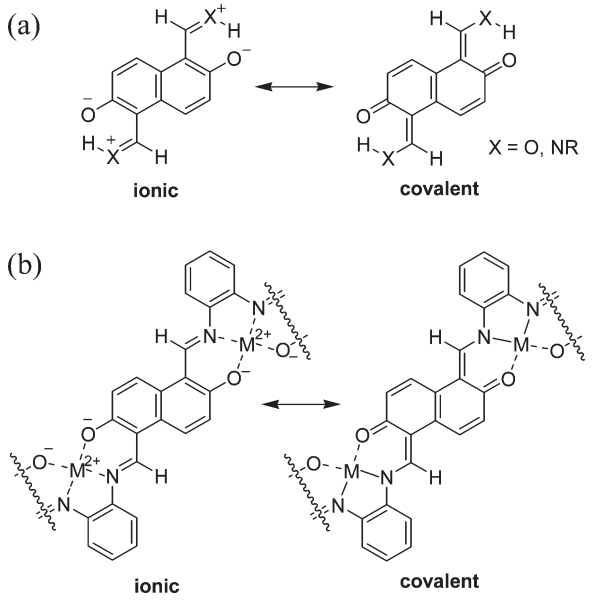

shown in Figure 3. In addition, we can predict how metal ions could influence the absorption properties of the naphthalene moiety: Scheme 3b implies that the metal ions' electronegativity, number of d-electrons, and oxidation number might affect the ratio of contributions from the ionic and covalent structures to the ground state's wave function. Namely, a more electronegative, and highly oxidized metal ion with fewer d-electrons, would induce a covalent interaction with chelating atoms, thus increasing the covalent character of the ground state structure. The chemical structure in Scheme 3 suggests that the π-conjugation is collapsed at nitrogen atoms for the complex in the covalent state. In this regard, the relatively low electronegativity (Pauling's value: Ni 1.91, Zn 1.65) of zinc would have increased the ionic character in the ground state, which might have resulted in the incomplete compartmentalization of the homo zinc triad as compared with the homo nickel triad.

Quantum Chemical Analysis. As discussed in the above section, the present di- and trinuclear complexes of the fused salphen ligand exhibit similar spectroscopic features as follows: (1) an intense absorption near 400 nm that is innate to the salphen moiety; (2) a moderate absorption near 500−600 nm that is innate to the bis-metalated 2,6-dihydroxynaphthalene; (3) relative intensities of these two bands that are roughly proportional to the number of the respective moieties contained in each molecule. These results suggest that the π-conjugated system can be divided into several compartments, each of which independently undergoes excitation. This picture is, at first glance, inconsistent with an empirical relationship between the elongation of π-conjugation and absorption maximum. One classical interpretation of this phenomenon is given by Scheme 3, which indicates that various Kekulé structures can be drawn independently for each salicylaldehyde Schiff-base moiety. In this section, we describe a more modern interpretation supported by a theoretical background.

We optimized the geometries of the dinuclear and trinuclear nickel complexes, for which alkyl chains were truncated to methyl groups for the sake of computational efficiency. We accepted

Table 2. Selected Data for the Results of SCI Calculation of Di- and Trinuclear Salphen Complexes

	$\lambda_{calcd.}$/nm (state)	dominant contributions (CI coefficients)	oscillator strength	$\lambda_{obsd.}$/nm
Ni_2L2	464 (^1B_u)	143→146 (−0.20)	0.56	580
		144→145 (0.60)		
	401 (^1B_u)	142→145 (−0.31)		
		142→147 (0.31)	1.10	
		143→146 (0.37)		401
	355 (^1B_u)	140→145 (0.39)	0.99	
		142→145 (−0.30)		
Ni_3L3	473 ($^1B_1$)	212→215 (−0.37)	0.68	
		213→214 (0.49)		
	452 ($^1A_1$)	212→214 (0.43)	0.49	583
		213→215 (−0.39)		
	408 ($^1A_1$)	210→214 (0.22)		
		210→216 (0.22)		
		211→215 (−0.22)	0.96	
		211→217 (0.22)		
		212→216 (0.23)		
	396 ($^1B_1$)	210→217 (0.29)	0.11	
		211→216 (0.30)		
	391 ($^1A_1$)	211→217 (0.23)		407
		212→218 (0.29)	0.27	
		213→219 (0.28)		
	361 ($^1B_1$)	207→214 (0.30)		
		208→215 (0.21)	1.52	
		209→214 (0.26)		
	352 ($^1A_1$)	207→215 (0.24)	0.34	
		209→215 (0.22)		

C_{2h} and C_{2v} structures as energy-minimum structures for Ni_2L2 and Ni_3L3, respectively, to simplify the subsequent orbital analysis, although those structures may not necessarily be global-minimum structures. Unfortunately, for similar complexes containing zinc atom(s), we could not achieve convergence of the structure under the conditions employed. For the optimized structures of nickel complexes, we calculated the absorption maxima using the ZINDO method.[31] Table 2 lists the calculated wavelengths selected for intense $\pi-\pi^*$ excitations, the electronic configurations and dominant contributions to the corresponding excited state, the oscillator strengths, and plausible assignments to experimentally observed wavelengths. Using these data, we simulated the absorption profiles of Ni_2L2 and Ni_3L3 (Supporting Information, Figure S4). Although the simulation qualitatively reproduced the observed profiles, the calculation underestimated the wavelengths of absorption maxima. In view of the limitation of the approximation used, the discussion should be confined to a semiquantitative level with respect to the reproduction of the wavelength.

For Ni_2L2, the absorption at 580 nm was assigned to the lowest $\pi-\pi^*$ excitation that is characterized by transition from #144(HOMO) to #145(LUMO) orbitals. The broad, intense band around 401 nm was assumed to include two modes of excitation, which are represented by transitions between near-HOMOs and near-LUMOs. For Ni_3L3, the absorption at 583 nm was assumed to include two modes of excitation, which are

dx.doi.org/10.1021/ic200798d |*Inorg. Chem.* 2011, 50, 5298–5306

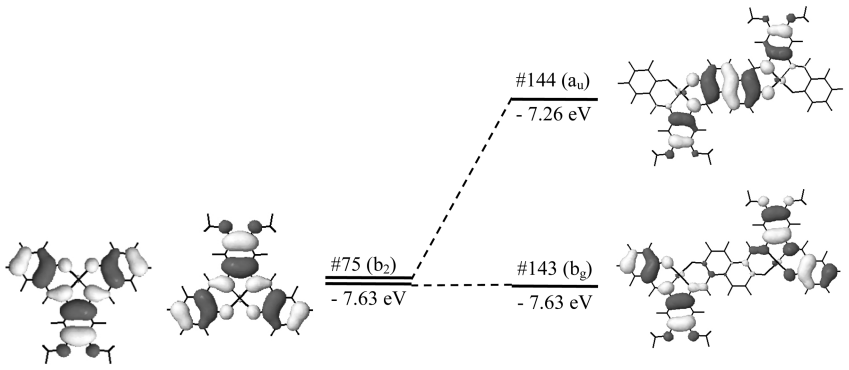

Figure 4. Schematic representation of interorbital interaction that generates near-HOMO orbitals of Ni_2L2.

characterized by transitions from #212(HOMO-1) or #213-(HOMO) to #214(LUMO) or #215(LUMO+1). The band around 407 nm was assumed to include five modes of excitation, which are represented by transitions between near-HOMOs and near-LUMOs. Note that the summed oscillator strength of the lower-energy band calculated for Ni_3L3 was 1.17 (= 0.68 + 0.49), which is roughly twice the corresponding value (0.56) calculated for Ni_2L2. This result is consistent with the observation that the intensity of each band was roughly proportional to the number of naphthalene moieties in the respective molecules. In addition, the summed oscillator strength of the higher-energy band calculated for Ni_3L3 was 3.20 (= 0.96 + 0.11 + 0.27 + 1.52 + 0.34), which is roughly 1.5 times the corresponding value (2.09) calculated for Ni_2L2. This ratio is also consistent with the observation that the intensity of this band is roughly proportional to the number of salphen moieties present in the respective molecule.

To gain further insight into the effect of elongated π-conjugation, we compared the orbital energy and spatial extent of near-HOMOs and near-LUMOs relevant to the observed $\pi-\pi^*$ transitions for nickel triads. As shown in Figure 4, #144 orbital (HOMO) of the dinuclear complex is localized at the central naphthalene moiety, that is, compartment B in Figure 1, and the shape of the nodules is reminiscent of the HOMO of 2,6-dihydroxynaphthalene-1, 5-carbaldehyde. On the other hand, #143 orbital (HOMO-1) is localized at the terminal salphen moieties (compartment A in Figure 1). The spatial extents of #144 and #143 orbitals correspond to symmetric and antisymmetric combinations of the salphen #75 (HOMO), respectively. From Figure 4, we can estimate the coupling constant to be about 0.4 eV. Similarly, #145 (LUMO) and #146 (LUMO+1) orbitals are regarded as results of antisymmetric and symmetric combinations of the salphen's #76 orbital (LUMO), respectively, and the coupling constant is 0.32 eV. These interorbital interactions raised the HOMO and lowered the LUMO, which in turn resulted in the appearance of the absorption band at 500−600 nm.

A similar analysis was applied to the near-HOMOs and near-LUMOs of the trinuclear complexes. Figure 5 illustrates the correlation diagram of the molecular orbitals between di- and trinuclear nickel complexes. Notably, the #212−#215 orbitals of Ni_3L3 are localized at the naphthalene moieties (i.e., compartments B and C). The #212 and #213 orbitals can be regarded as the antisymmetric and symmetric combination of the naphthalene HOMO, respectively, and the former is more stable than the latter by 0.07 eV. Similarly, the coupling of naphthalene's LUMO resulted in the #214 and #215 orbitals, which are separated by 0.13 eV. These splitting values for the naphthalene orbital are small compared to those of the interorbital interaction between the salphen orbitals, indicating that the salphen's metal coordination site effectively breaks the π-conjugation in the complex. The splitting of the orbitals results in two possible modes of excitation that lead to $^1B_1$ and $^1A_1$ states, but the corresponding absorption peaks overlap each other in one slightly broadened band because of the small difference in excitation energy between these states. Consequently, it is suggested that because of the small interorbital coupling through the coordination sites, the absorption spectra can be interpretable as a sum of contributions from each of compartmentalized π-conjugated systems.

The orbitals that give rise to the higher-energy absorption band, are rather localized around the terminal salphen complex moieties (i.e., compartment A). As shown in Supporting Information, Figure S5, Orbitals #142 and #143 of Ni_2L2 can be regarded as the symmetric and antisymmetric combinations of the salphen HOMO, respectively, and the former is more stable than the latter by 0.06 eV by virtue of coupling with the next-HOMO-type orbital of the naphthalene moiety. This splitting is also regarded as a result of the interorbital interaction between two salphen moieties when they are fused into a naphthalene ring. Similarly, orbitals #146 and #147 are the symmetric and antisymmetric combinations of the salphen LUMO, respectively. The transitions among those four orbitals (#142, #143, #146, and #147) result in two ^1B_u excited states, which can be classically interpreted as two salphen moieties individually undergoing electronic excitation. For Ni_3L3, although the situation is more complicated, the transitions among six orbitals (#209−211 and #216−218) result in three $^1A_1$ states and two $^1B_1$ states, which can be classically interpreted as three salphen moieties individually undergoing electronic excitation (Supporting Information, Figure S5).

To investigate the effect of changing metal ion(s) on the electronic structure, we performed similar ZINDO calculations for the molecular structures of some heterotrinuclear complexes that were obtained by replacing the nickel atom with another metal. Although the geometry optimization of those structures was not successful, the computational results would rather highlight the net effect originating from metal ion. The calculated excitation energies that correspond to the observed absorption maxima were not substantially affected by the combination of metal atoms, namely, Ni−Ni−Ni, Ni−Zn−Ni, and Zn−Zn−Zn triads. These results are quite reasonable since those excitations have few contributions of d-orbitals, and are in agreement with the experimental results. The shape of the nodules of near-HOMO

dx.doi.org/10.1021/ic200798d |*Inorg. Chem.* 2011, 50, 5298–5306

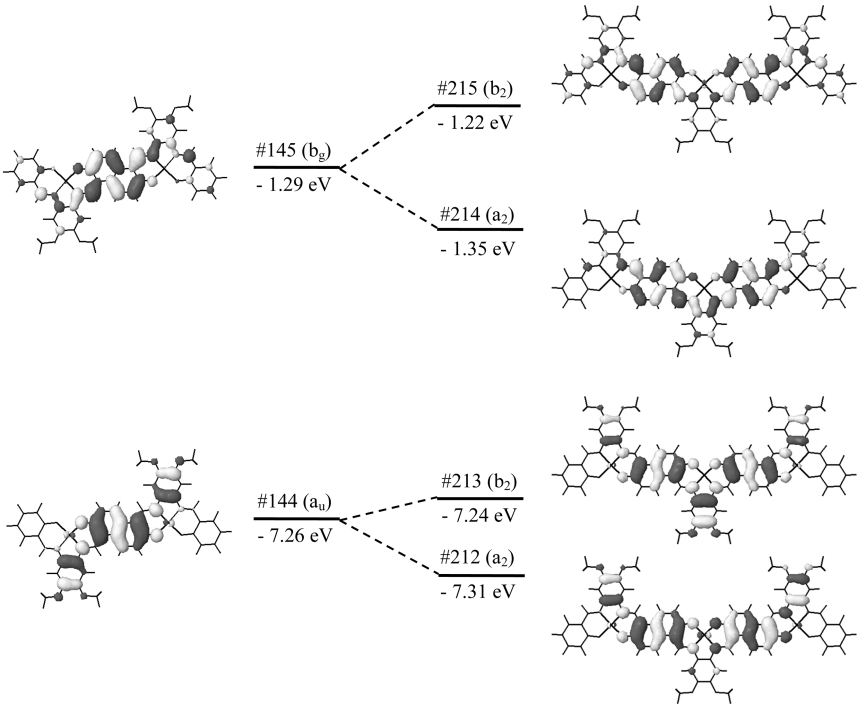

Figure 5. Schematic representation of the correlation diagram of the near-HOMO/LUMO orbitals between di- and trinuclear nickel complexes.

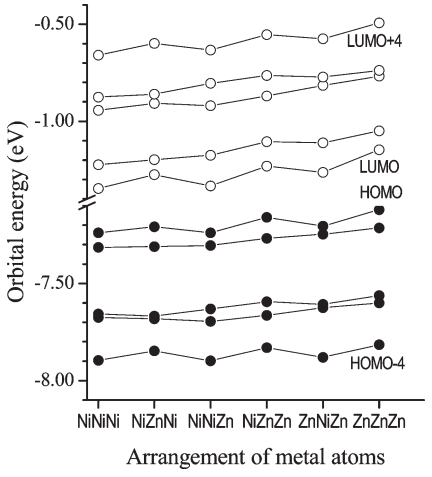

Figure 6. Orbital energies of several occupied (●) and vacant (○) orbitals near HOMO and LUMO, as a function of the arrangement of metals in Ni/Zn trinuclear complexes.

and near-LUMO orbitals was essentially identical among three arrangements of metal atoms. However, the orbital energies of those orbitals were appreciably changed depending on the arrangement. Figure 6 shows the energy of selected orbitals for the possible combinations of nickel and zinc atoms. It is notable that the energy difference between HOMO and HOMO-1 is significantly larger for Ni−Zn−Ni, Ni−Zn−Zn, and Zn−Zn−Zn triads than for the others, indicating that the central zinc atom increases interorbital interactions between naphthalene's HOMO-like orbitals on the both sides. This tendency is in agreement with the consideration based on resonance hybrid (Scheme 3). In contrast, the energy difference between LUMO and LUMO+1 shows an opposite tendency. The apparent degeneracy between HOMO-2 and HOMO-3 and between LUMO+2 and LUMO+3 is resolved for asymmetric triads, that is, Ni−Ni−Zn and Ni−Zn−Zn, consistent with these orbitals being localized at the terminal salphen moieties. Although the level of approximation is not sufficient for quantitative discussion, the present calculations strongly suggest that the combination of metal atoms significantly affects the electronic state of the fused salphen triad. Consequently, it is expected that the choice of metal ion(s) with various properties such as electronegativity, the number of d-electrons, and oxidation number could tune the electronic communication between π-conjugated systems through a salphen unit.

CONCLUSIONS

Utilizing a stepwise condensation reaction of 2,6-dihydroxy-1,5-dicarbaldehyde, we have prepared a series of homo- and heteronuclear triads embedded into a π-conjugated fused salphen ligand. These compounds not only are attractive in their shape-persistence, but also provided us with comprehensive information on the effects of an extended π-conjugated system on the absorption properties of salphen complexes. Comparison of the trinuclear complexes' spectroscopic features with those of analogous dinuclear complexes revealed that the absorption spectra of the trinuclear complexes are composed of a salphen-centered absorption band at 400 nm and a naphthalene-centered absorption band around 500−600 nm. This observation suggests that the π-conjugated system is divided into several compartments, each of which independently undergoes electronic excitation. This compartmentalization was more clearly observed for nickel complexes than for zinc complexes. Close analysis of the results of molecular orbital calculations revealed that interactions mediated by the naphthalene ring between the coordination sites are appreciably large. These interactions were interpretable as interorbital interactions resulting from the formal fusion of benzene rings into a naphthalene ring. However, the N_2O_2 metal

dx.doi.org/10.1021/ic200798d |*Inorg. Chem.* 2011, 50, 5298–5306

coordination site effectively breaks electronic communication by breaking the π-conjugation, even though the site is bridged by an *o*-phenylene linkage. These results may demand reconsideration of the molecular design of π-conjugated metallo-polysalen/-salphens. Specifically, to make full use of conjugated systems for improving various electronic and optical properties in these complexes, further consideration should be given to the design of the coordination site, including bridge(s) and metal(s), as well as that of the linker moiety. For example, chemical or electrochemical treatment could change the oxidation state of the coordination site, which could increase or decrease the number of π-electrons and thus change the nature of the interorbital interactions between the two halves of the salphen moiety through the coordination site.

■ ASSOCIATED CONTENT

Supporting Information. Supplementary ^{1}H NMR spectra, some computational results, and the numerical data of optimized geometry calculated for the compounds studied. This material is available free of charge via the Internet at http://pubs.acs.org.

■ AUTHOR INFORMATION

Corresponding Author

*Phone: +81-3-5452-6367. Fax: +81-3-5452-6366. E-mail: houjou@iis.u-tokyo.ac.jp.

■ REFERENCES

(1) Abd-El-Aziz, A. S., Carraher, C. E., Jr., Pittman, C. U., Jr., Zeldin, M., Eds.; . In *Metal-coordination polymers*; John Wiley & Sons, Inc.: Hoboken, NJ, 2005; Vol. 5.

(2) Whittell, G. R.; Manners, I. *Adv. Mater.* **2007**, *19*, 3439.

(3) Leung, A. C. W.; Maclachlan, M. J. *J. Inorg. Organomet. Polym. Mater.* **2007**, *17*, 57.

(4) Hofmeier, H.; Schubert, U. S. *Chem. Commun.* **2005**, 2423.

(5) Hirao, T. *Coord. Chem. Rev.* **2002**, *226*, 81.

(6) Holiday, B. J.; Swager, T. M. *Chem. Commun.* **2005**, 23.

(7) Pickup, P. G. *J. Mater. Chem.* **1999**, *9*, 1641.

(8) O'Sullivan, T. J.; Djukic, B.; Dube, P. A.; Lemaire, M. T. *Chem. Commun.* **2009**, 1903.

(9) Masui, H. *Coord. Chem. Rev.* **2001**, *219*−*221*, 957.

(10) Evangelio, E.; Ruiz-Molina, D. *Eur. J. Inorg. Chem.* **2005**, 2957.

(11) (a) Shimazaki, Y.; Tani, F.; Fukui, K.; Naruta, Y.; Yamauchi, O. *J. Am. Chem. Soc.* **2003**, *125*, 10512. (b) Shimazaki, Y.; Kabe, R.; Huth, S.; Tani, F.; Naruta, Y.; Yamauchi, O. *Inorg. Chem.* **2007**, *46*, 6083.

(12) Sato, O.; Tao, J.; Zhang, Y.-Z. *Angew. Chem., Int. Ed.* **2007**, *46*, 2152.

(13) Borisova, N. E.; Reshetova, M. D.; Ustynyuk, Y. A. *Chem. Rev.* **2007**, *107*, 46.

(14) Dai, Y.; Katz, T. J. *J. Org. Chem.* **1997**, *62*, 1274. Dai, Y.; Katz, T. J.; Nicholas, D. A. *Angew. Chem., Int. Ed. Engl.* **1996**, *35*, 2109.

(15) (a) Akine, S.; Hashimoto, D.; Saiki, T.; Nabeshima, T. *Tetrahedron Lett.* **2004**, *45*, 4225. (b) Nabeshima, T.; Miyazaki, H.; Iwasaki, A.; Akine, S.; Saiki, T.; Ikeda, C. *Tetrahedron* **2007**, *63*, 3328.

(16) (a) Hui, K.-H. J.; MacLachlan, M. J. *Chem. Commun.* **2006**, 2480. (b) Gallant, A. J.; Hui, J. K.-H.; Zahariev, F. E.; Wang, Y. A.; MacLachlan, M. J. *J. Org. Chem.* **2005**, *70*, 7936. (c) Gallant, A.; Yun, M.; Sauer, M.; Yeung, C. S.; MacLachlan, M. J. *Org. Lett.* **2005**, *7*, 4827.

(17) (a) Rotthaus, O.; Thomas, F.; Jarjayes, O.; Philouze, C.; Saint-Aman, E.; Pierre, J.-L. *Chem.—Eur. J.* **2006**, *12*, 6953. (b) Rotthaus, O.; Jarjayes, O.; Philouze, C.; Del Valle, C. P.; Thomas, F. *Chem. Commun.* **2009**, 1792. (c) Rotthaus, O.; Jarjayes, O.; Philouze, C.; Pérez Del Valle, C.; Thomas, F. *Dalton Trans.* **2009**, 1792.

(18) (a) Glaser, T.; Heidemeier, M.; Fröhlich, R.; Hildebrandt, P.; Bothe, E.; Bill, E. *Inorg. Chem.* **2005**, *44*, 5467. (b) Theil, H.; von Richthofen, C.-G. F.; Stammler, A.; Bögge, H.; Glaser., T. *Inorg. Chim. Acta* **2008**, *361*, 916. (c) Glaser, T.; Heidemeier, M.; Strautmann, J. B. H.; Bögge, H.; Stammler, A.; Krickemeyer, E.; Huenerbein, R.; Grimme, S.; Bothe, E.; Bill, E. *Chem.—Eur. J.* **2005**, *44*, 5467. (d) Glaser, T.; Heidemeier, M.; Krickemeyer, E.; Bögge, H.; Stammler, A.; Fröhlich, R.; Bill, E.; Schnack, J. *Inorg. Chem.* **2009**, *48*, 607.

(19) (a) Kleij, A. W. *Eur. J. Inorg. Chem.* **2009**, 193. (b) Crreli, S.; Escudero-Adan, E. C.; Benet-Buchholz, J.; Kleij, A. W. *Eur. J. Inorg. Chem.* **2008**, 2863. (c) Escudero-Adan, E. C.; Benet-Buchholz, J.; Kleij, A. W. *Inorg. Chem.* **2007**, *46*, 7265. (d) Wezenberg, S. J.; Kleij, A. W. *Org. Lett.* **2008**, *10*, 3311.

(20) Manecke, G.; Wille, W. E. *Makromol. Chem.* **1970**, *133*, 61. Maneke, G.; Wille, W. E. *G. Kossmehl, Makromol. Chem.* **1972**, *160*, 111.

(21) Leung, A. C. W.; Hui, J. K.−H.; Chong, J. H.; Maclachlan, M. J. *Dalton Trans.* **2009**, 5199–5210.

(22) (a) Leung, A. C. W.; Chong, J. H.; Patrick, B. O.; MacLachlan, M. J. *Macromolecules* **2003**, *36*, 5051. (b) Leung, A. C. W.; MacLachlan, M. J. *J. Mater. Chem.* **2007**, *17*, 1923.

(23) (a) Goldsby, K. A. *J. Coord. Chem.* **1988**, *19*, 83. (b) Audebert, P.; Capdevielle, P.; Maumy, M. *New J. Chem.* **1991**, *15*, 235. (c) Dahm, C. E.; Peters, D. G. *Anal. Chem.* **1994**, *66*, 3117. (d) Vilas-Boas, M.; Freire, C.; de Castro, B.; Christensen, P. A.; Hillman, A. R. *Inorg. Chem.* **1997**, *36*, 4919.

(24) (a) Kingsborough, R. P.; Swager, T. M. *J. Am. Chem. Soc.* **1999**, *121*, 8825. (b) Kingsborough, R. P.; Swager, T. M. *Adv. Mater.* **1998**, *14*, 110.

(25) (a) Houjou, H.; Sasaki, T.; Shimizu, Y.; Koshizaki, N.; Kanesato, M. *Adv. Mater.* **2005**, *17*, 606. (b) Houjou, H.; Shimizu, Y.; Koshizaki, N.; Kanesato, M. *Adv. Mater.* **2003**, *15*, 1458.

(26) Houjou, H.; Motoyama, T.; Banno, S.; Yoshikawa, I.; Araki, K. *J. Org. Chem.* **2009**, *74*, 520.

(27) Dewer, M. J. S.; Talati, A. M. *J. Am. Chem. Soc.* **1963**, *85*, 1874. Dewer, M. J. S.; Talati, A. M. *J. Am. Chem. Soc.* **1963**, *86*, 1592.

(28) (a) Houjou, H.; Motoyama, T.; Araki, K. *Eur. J. Inorg. Chem.* **2009**, 533. (b) Houjou, H.; Ito, M.; Araki, K. *Inorg. Chem.* **2009**, *48*, 10703.

(29) Rosa, D. T.; Reynolds, R. A., III; Malinak, S. M.; Coucouvanis, D. *Inorg. Synth.* **2002**, *33*, 112.

(30) Frisch, M. J.; Trucks, G. W.; Schlegel, H. B.; Scuseria, G. E.; Robb, M. A.; Cheeseman, J. R.; Montgomery, J. A.; , Jr., Vreven, T.; Kudin, K. N.; Burant, J. C.; Millam, J. M.; Iyengar, S. S.; Tomasi, J.; Barone, V.; Mennucci, B.; Cossi, M.; Scalmani, G.; Rega, N.; Petersson, G. A.; Nakatsuji, H.; Hada, M.; Ehara, M.; Toyota, K.; Fukuda, R.; Hasegawa, J.; Ishida, M.; Nakajima, T.; Honda, Y.; Kitao, O.; Nakai, H.; Klene, M.; Li, X.; Knox, J. E.; Hratchian, H. P.; Cross, J. B.; Adamo, C.; Jaramillo, J.; Gomperts, R.; Stratmann, R. E.; Yazyev, O.; Austin, A. J.; Cammi, R.; Pomelli, C.; Ochterski, J. W.; Ayala, P. Y.; Morokuma, K.; Voth, G. A.; Salvador, P.; Dannenberg, J. J.; Zakrzewski, V. G.; Dapprich, S.; Daniels, A. D.; Strain, M. C.; Farkas, O.; Malick, D. K.; Rabuck, A. D.; Raghavachari, K.; Foresman, J. B.; Ortiz, J. V.; Cui, Q.; Baboul, A. G.; Clifford, S.; Cioslowski, J.; Stefanov, B. B.; Liu, G.; Liashenko, A.; Piskorz, P.; Komaromi, I.; Martin, R. L.; Fox, D. J.; Keith, T.; M. A. Al-Laham, Peng, C. Y.; Nanayakkara, A.; Challacombe, M.; Gill, P. M. W.; Johnson, B.; Chen, W.; Wong, M. W.; Gonzalez, C.; Pople, J. A. *Gaussian 03*, Revision C.02; Gaussian, Inc.: Wallingford, CT, 2004.

(31) Zerner, M. C. In *Reviews in Computational Chemistry*; Lipkowitz, K. B., Boyd, D. B., Eds.; VCH: New York, 1991; Vol. 2, p 313.

(32) Maynau, D.; Heully, J.-L. *Chem. Phys. Lett.* **1991**, *187*, 295.

(33) *Jmol: an open-source Java viewer for chemical structures in 3D*; http://www.jmol.org/.

(34) Gilli, G.; Bellucci, F.; Ferretti, V.; Bertolasi, V. *J. Am. Chem. Soc.* **1989**, *111*, 1023.

(35) Sobczyk, L.; Grabowski, S. J.; Krygowski, T. M. *Chem. Rev.* **2005**, *105*, 3513.

(36) (a) Sanz, P.; Mó, O.; Yáñez, M.; Elguero, J. *ChemPhysChem* **2007**, *8*, 1950. (b) Sanz, P.; Mó, O.; Yáñez, M.; Elguero, J. *J. Phys. Chem. A* **2007**, *111*, 3585. (c) Sanz, P.; Mó, O.; Yáñez, M.; Elguero, J. *Chem.—Eur. J.* **2008**, *14*, 4225.

(37) (a) Palusiak, M.; Simon, S.; Solà, M. *J. Org. Chem.* **2006**, *71*, 5241. (b) Krygowski, T. M.; Zachara-Horeglad, J. E.; Palusiak, M.; Pelloni, S.; Lazzeretti, P. *J. Org. Chem.* **2008**, *73*, 2138.

(38) Dobosz, R.; Skotnicka, A.; Rozwadowski, Z.; Dziembowska, T.; Gawinecki, R. *J. Mol. Struct.* **2010**, *979*, 194.

(39) (a) Krygowski, T. M.; Zachara, J. E.; Ośmiałowski, B.; Gawinecki, R. *J. Org. Chem.* **2006**, *71*, 7678. (b) Krygowski, T. M.; Zachara-Horeglad, J. E.; Palusiak, M. *J. Org. Chem.* **2010**, *75*, 4944.

(40) Karabiyik, H.; Erdem, Ö.; Aygün, M.; Güzel, B.; García-Granda, S. *J. Inorg. Organomet. Polym.* **2010**, *20*, 142.